

RESEARCH

Open Access



# A novel model for predicting immunotherapy response and prognosis in NSCLC patients

Ting Zang<sup>1†</sup>, Xiaorong Luo<sup>1†</sup>, Yangyu Mo<sup>1</sup>, Jietao Lin<sup>2,3</sup>, Weiguo Lu<sup>2</sup>, Zhiling Li<sup>4\*</sup>, Yingchun Zhou<sup>2,3\*</sup> and Shulin Chen<sup>4\*</sup>

## Abstract

**Background** How to screen beneficiary populations has always been a clinical challenge in the treatment of non-small-cell lung cancer (NSCLC) with immune checkpoint inhibitors (ICIs). Routine blood tests, due to their advantages of being minimally invasive, convenient, and capable of reflecting tumor dynamic changes, have potential value in predicting the efficacy of ICIs treatment. However, there are few models based on routine blood tests to predict the efficacy and prognosis of immunotherapy.

**Methods** Patients were randomly divided into training cohort and validation cohort at a ratio of 2:1. The random forest algorithm was applied to select important variables based on routine blood tests, and a random forest (RF) model was constructed to predict the efficacy and prognosis of ICIs treatment. For efficacy prediction, we assessed receiver operating characteristic (ROC) curves, decision curve analysis (DCA) curves, clinical impact curve (CIC), integrated discrimination improvement (IDI) and net reclassification improvement (NRI) compared with the Nomogram model. For prognostic evaluation, we utilized the C-index and time-dependent C-index compared with the Nomogram model, Lung Immune Prognostic Index (LIPI) and Systemic Inflammatory Score (SIS). Patients were classified into high-risk and low-risk groups based on RF model, then the Kaplan–Meier (K–M) curve was used to analyze the differences in progression-free survival (PFS) and overall survival (OS) of patients between the two groups.

**Results** The RF model incorporated RDW-SD, MCV, PDW, CD3<sup>+</sup>CD8<sup>+</sup>, APTT, P-LCR, Ca, MPV, CD4<sup>+</sup>/CD8<sup>+</sup> ratio, and AST. In the training and validation cohorts, the RF model exhibited an AUC of 1.000 and 0.864, and sensitivity/specificity of (100.0%, 100.0%) and (70.3%, 93.5%), respectively, which had superior performance compared to the Nomogram model (training cohort: AUC = 0.531, validation cohort: AUC = 0.552). The C-index of the RF model was 0.803 in the training cohort and 0.712 in the validation cohort, which was significantly higher than Nomogram model, LIPI and SIS. K-M survival curves revealed that patients in the high-risk group had significantly shorter PFS/OS than those in the low-risk group.

<sup>†</sup>Ting Zang and Xiaorong Luo are co-first authors.

\*Correspondence:

Zhiling Li

lizhl@sysucc.org.cn

Yingchun Zhou

yingchunbaby@126.com

Shulin Chen

chenshl@sysucc.org.cn

Full list of author information is available at the end of the article



**Conclusions** In this study, we developed a novel model (RF model) to predict the response to immunotherapy and prognosis in NSCLC patients. The RF model demonstrated better predictive performance for immunotherapy responses than the Nomogram model. Moreover, when predicting the prognosis of immunotherapy, it outperformed the Nomogram model, LIPI, and SIS.

**Keywords** Non-small cell lung cancer, Predictive biomarkers, Immune checkpoint inhibitors, Machine learning

## Introduction

Lung cancer holds the position as the second most frequent malignancy and represents the predominant factor in cancer-related death worldwide. Also, it is the most prevalent and fatal cancer in China, imposing a significant burden on both the global economy and healthcare systems [1]. Lung cancer is primarily classified into two pathological types: non-small cell lung cancer (NSCLC) and small cell lung cancer (SCLC), with NSCLC comprising approximately 85% of total diagnoses [2]. Tumor immunotherapy encompasses a range of therapeutic strategies, including immune checkpoint inhibitors (ICIs), which typically target programmed cell death receptor 1 (PD-1), programmed cell death ligand 1 (PD-L1), and cytotoxic T lymphocyte-associated antigen 4 (CTLA-4). These therapies exert their antitumor effects by modulating T-cell-mediated immune responses [3]. The ICIs treatment has revolutionized the therapeutic paradigms for various malignancies, including melanoma [4], head and neck cancer (HNC) [5], bladder cancer [6], kidney cancer [7], and NSCLC [8].

ICIs have emerged as a first-line treatment option for lung cancer, especially for NSCLC, either as monotherapy or in combination with radiotherapy, chemotherapy, and targeted therapies in clinical guidelines [9]. However, not all NSCLC patients benefit from ICIs, with only about 20–30% of them achieving significant clinical improvement [10]. Currently, the quantification of PD-L1 expression remains the standard method in clinic for identifying patients who benefit from immunotherapy. However, the predictive accuracy of PD-L1 as an ICIs response biomarker continues to face inconsistencies and ongoing debates, with variability in detection antibodies, interpretation criteria and threshold selection [11]. Furthermore, tumor mutational burden (TMB) has also been determined as a key biomarker for predicting responses to immunotherapy [12]. Nevertheless, the lack of standardized assessment criteria [12] and the high costs of testing limit its application in routine clinical practice. With advancements in high-throughput multiplex testing, a variety of immune predictive biomarkers based on peripheral blood have been identified. Plasma exosomal miRNA profiles, such as hsa-miR-320b, hsa-miR-320c, have been found as potential ICIs efficacy biomarkers in NSCLC [13]. Soluble factors, particularly interleukin-6

(IL-6), have been studied as predictive and prognostic factors for ICIs response [14, 15]. Circulating tumor DNA (ctDNA) reflects real-time tumor cell death. Due to the complexity of the techniques involved and high cost, ctDNA remains far from being fully integrated into routine clinical practice.

Therefore, there is an acute need to develop new approaches to help clinicians predict the prognosis and response to Immunotherapy in patients. Here, we constructed a clinical prediction model to assess the clinical response of NSCLC patients to ICIs therapy, aiming to assist clinicians in selecting patients most prone to benefit.

It is well established that the presence, activation, and stimulation of various components of the immune system, such as T cells, B cells and natural killer (NK) cells, are essential for antitumor immune response [16]. Emerging evidence reveals that the response to ICIs is associated with the quality and intensity of T cell, NK cell, and B cell responses whether in the tumor microenvironment (TME) [17] or peripheral blood [18]. Tumors can be classified into three basic immune phenotypes: immune-inflamed, immune-excluded, and immune-desert, based on the distribution of cytotoxic immune cells within the TME [19]. Immune-inflamed tumors, also referred to as hot tumors, are characterized by high levels of T cell infiltrates, enhanced signaling of interferon-gamma (IFN- $\gamma$ ), increased expression of PD-L1, and a high TMB [20]. Hot tumors are often more sensitive to ICIs [21, 22]. In contrast, immune-excluded and immune-desert tumors, known as cold tumors, are characterized by poor CD8<sup>+</sup> T lymphocyte infiltration, low mutational burden, low expression of major histocompatibility complex (MHC) class I, and low PD-L1 expression [20]. The anti-tumor response mediated by ICIs depends on the expression of PD-L1 in the tumor and the infiltration of T cells capable of recognizing and destroying tumor cells. One study suggested [23] that pathological examinations show patients exhibiting a high density of CD8<sup>+</sup> T cells within tumor tissue (classified as hot tumors with  $\geq 12.0$ /field) have a better progression-free survival (PFS) during immunotherapy than those with a lower frequency (cold tumors:  $< 12.0$ /field). Common hot tumors include NSCLC [24], melanoma [25], renal cell carcinoma [26], and head and neck squamous cell carcinoma [27], while common cold

tumors include pancreatic cancer [28], glioblastoma [29], and prostate cancer [30]. In tumor treatment, hot tumors have demonstrated a favorable immune response.

To the best of our knowledge, few studies have explored predictive models that integrate absolute counts of lymphocyte subpopulations with other routine blood tests for predicting immunotherapy response and prognosis in NSCLC patients. In this study, we utilized routine blood tests to construct a novel model to evaluate therapeutic efficacy and prognosis in NSCLC patients, with the aim of assisting clinicians in identifying patients benefiting from ICIs therapy.

## Materials and methods

### Patients

A retrospective study included 319 patients with NSCLC who received ICIs therapy between November 16, 2016, and December 29, 2022, at Sun Yat-sen University Cancer Center. The deadline for follow-up was September 2024. For the patients who were included in the study, the criteria for inclusion and exclusion were established as follows: (1) pathologically confirmed diagnosis of NSCLC (stage I–IV); (2) age over 18 years; (3) received ICIs therapy; (4) baseline assessments were performed with a CT scan of the chest and abdomen, MRI of the head within 2 weeks before treatment, subsequently the oncological outcomes were evaluated after every two cycles of treatment; (5) Complete blood count, biochemical indexes, lymphocyte subpopulations, and other routine blood tests were measured before the first ICIs treatment; (6) patients who lacked any required blood examination results or lost to follow-up were excluded.

Patients were randomly divided into training and validation cohorts at a ratio of 2:1. The training cohort was utilized to develop the predictive model, while the validation cohort served to assess its performance. Responses of immunotherapy were assessed according to the response evaluation criteria in solid tumors (RECIST) 1.1. based on CT or MRI results. Efficacy of immunotherapy was categorized as complete response (CR), partial response (PR), stable disease (SD), or progressive disease (PD). CR indicates total tumor disappearance with no residual tumor in primary and metastatic sites. PR is defined as a reduction in tumor volume of  $\geq 30\%$ , with all lesions shrinking. SD signifies no significant increase in tumor size ( $< 20\%$ ) and no new lesions, while PD is characterized by a  $\geq 20\%$  increase in tumor volume or the emergence of new lesions. Overall survival (OS) was defined as the duration from the start of immunotherapy to any cause of death (or last follow-up). PFS was measured from the beginning of immunotherapy to the earliest of disease progression or death.

### Data collection

All clinical information and experimental data of patients were collected from the electronic medical record system. The obtained data included clinical characteristics (sex, age, KPS score, histological type, TNM stage, clinical stage, treatment and outcomes, etc.), complete blood count, biochemical indicators, lymphocyte subsets counts, and inflammatory markers.

### Laboratory measurements

Serum and plasma samples were acquired before the baseline visit and subsequently centrifuged for 10 min at 3500 r/min. All biomarkers were analyzed using commercially available reagents following the manufacturer's guidelines. Complete blood count was estimated using Sysmex XN 9000 (Japan). Coagulation test was assessed using Sysmex XN 5100 (Japan).

Biochemical indicators (renal function tests, liver function tests, Inflammation tests and blood lipid tests) were estimated using Hitachi 008 (Japan). Lymphocyte subsets analysis was performed with BD FACS Canto II (USA).

### Statistical analysis

Categorical data were analyzed using the Pearson  $\chi^2$  test or Fisher's exact test, while continuous variables were compared using the independent two-sample t-test or the Mann–Whitney U test. All statistical analyses were conducted using SPSS (version 29.0). Patients were randomly allocated to the training and validation cohorts. Using the random forest algorithm, we screened key variables associated with disease progression following immunotherapy and constructed a random forest efficacy prediction model. Additionally, the selected variables were employed to build a random forest prognosis model for tumors. The predictive performance of the random forest model (RF model) was compared with the Nomogram model [31], using receiver operating characteristic (ROC) curves and decision curve analysis (DCA). The Nomogram model [31] was constructed using four factors (liver metastasis, metastatic sites, APTT and Treg cells) by Wang et al. to predict the efficacy of NSCLC immunotherapy. Subsequently, the concordance index (C-index) and time-dependent c-index were used to compare the disease prognostic accuracy of the RF model, Nomogram model, Lung Immune Prognostic Index (LIPI) [32], and Systemic Inflammation Score (SIS) [33]. Based on the risk scores obtained from the RF model, patients in both the training cohort and the validation cohort were divided into low-risk and high-risk groups, respectively. The Kaplan–Meier (K–M) curve was applied to estimate OS and PFS, as well as to generate the survival curves for the Nomogram model, LIPI and SIS at different risk scores. Statistical tests used were two-sided, set at a

0.05 significance level, and *p* values <0.05 were regarded as statistically significant. Statistical analyses were conducted using R software (version 4.3.3).

## Results

### Patient characteristics

A total of 319 patients (260 men [81.50%]; 59 women [18.50%]; average age 58.7 years [range 18–81 years]) treated with ICIs at Sun Yat-sen University Cancer Center between 2016 and 2022 were included in this study. Clinicopathological variables, clinical characteristics, and complete blood count of patients in the training (n=214) and validation (n=105) cohorts are listed in Supplement table (S1–S2). No differences were observed between the two cohorts in terms of age, gender, pathological classification, KPS score, immunotherapy regimen, and clinical efficacy evaluation. Patients were distributed across stages I, II, III, and IV as follows: 2 (0.63%), 2 (0.63%), 192 (60.19%) and 123 (38.56%), respectively. The training cohort included 7 (3.27%) patients with CR and 66 (30.84%) with PR, while the validation cohort had 2 (1.90%) patients with CR and 42 (40%) with PR. The number of SD in the training and validation cohorts is 70 (32.71%) and 30 (28.57%), respectively. Additionally, 102 patients experienced PD, with 71 (33.18%) in the training and 31 (29.52%) in the validation cohort.

### Construction and evaluation of prediction model

In the training cohort, the random forest algorithm was used to identify the important predictor variables from peripheral blood-based biomarkers. We constructed a 10-prognostic index signature, consisting of red cell distribution width-standard deviation (RDW-SD), mean corpuscular volume (MCV), platelet distribution width (PDW), CD3<sup>+</sup>CD8<sup>+</sup>, activated partial thromboplastin time (APTT), platelet-large cell ratio (P-LCR), calcium (Ca), mean platelet volume (MPV), CD4<sup>+</sup>/CD8<sup>+</sup> ratio, and aspartate aminotransferase (AST). The Multi-way importance plot and variable importance ranking are presented in Fig. 1A, B, respectively.

### The model's performance in predicting the response to ICIs therapy

Here, we used the random forest algorithm to construct a predictive model for ICIs efficacy in NSCLC patients and compared its performance with the predictive Nomogram model. As shown in Fig. 2, we assessed the predictive accuracy of RF model by comparing the area under the curve (AUC) with the Nomogram model. The RF model achieved an AUC of 1.000 in the training cohort, significantly outperforming the Nomogram model (AUC: 0.531) (Fig. 2A). Similarly, in the validation cohort, the RF model maintained superior performance with an AUC of 0.864, compared to the Nomogram model (AUC: 0.552).

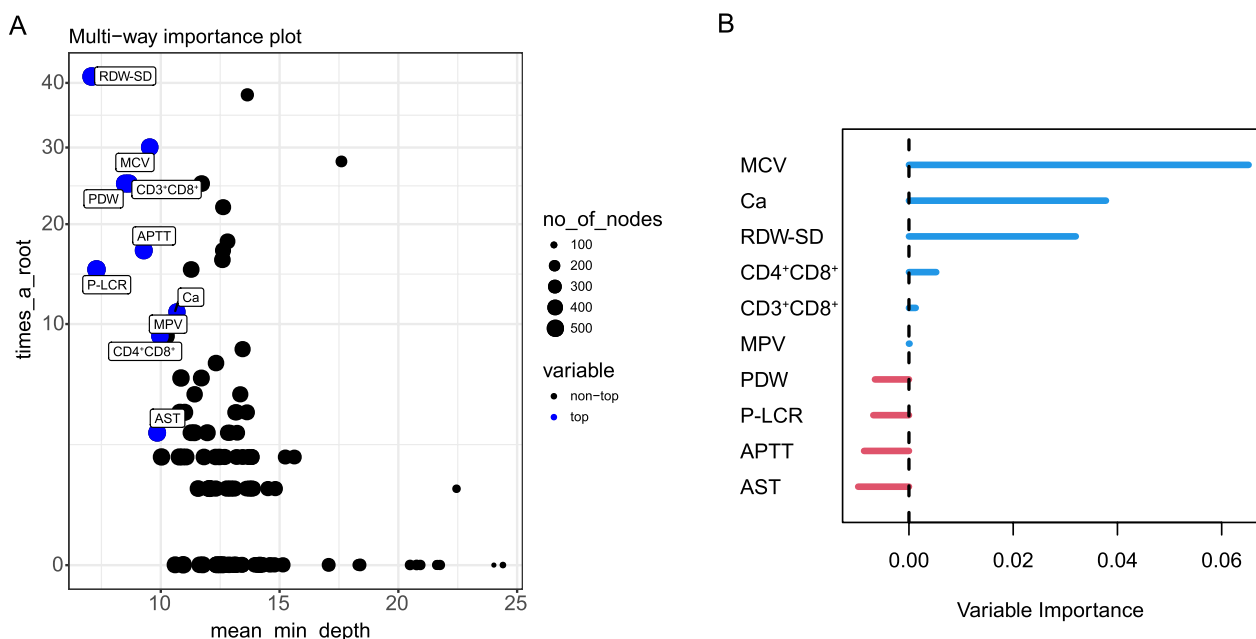


**Fig. 1** Development of a prognostic model based on blood indicators and baseline information using random forest algorithm. **A** Top 10 predictive variables associated with treatment outcomes selected from baseline clinical data. **B** Variable importance plot showing the contribution of each selected variable to the prognostic model

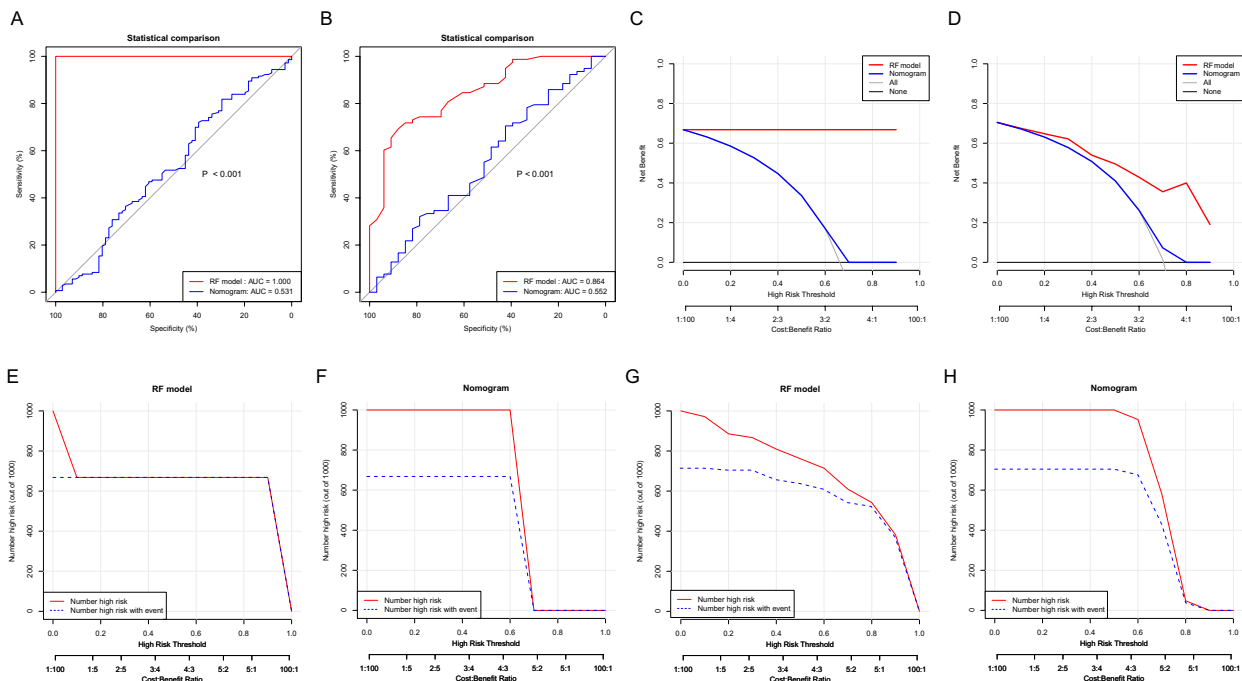


**Fig. 2** Comparison of predictive accuracy between the RF model and the Nomogram model for assessing ICIs efficacy in NSCLC patients. **A–B** ROC curves of the RF model and the Nomogram model in the training (**A**) and validation cohorts (**B**). **C–D** DCA for the RF model compared with the Nomogram model in the Training (**C**) and validation cohorts (**D**). The black horizontal line indicates the net benefit in the scenario where it is assumed that none of the NSCLC patients will experience any outcome. **E–H** CIC for the RF model and the Nomogram model. **E, F** show the training cohort and **G, H** shows the validation cohort. The red line, representing the count of high-risk individuals, shows the quantity of people the model categorizes as positive (high-risk) at every threshold probability. The blue line, denoting the number of high-risk individuals with actual positive outcomes, indicates the number of truly positive cases at each threshold probability

Regarding sensitivity and specificity, the RF model demonstrated 100.0% sensitivity and specificity in the training cohort, while the Nomogram model exhibited a sensitivity of 39.4% and specificity of 72.0%. In the validation cohort, the RF model achieved a sensitivity of 70.3% and specificity of 93.5%, whereas the Nomogram model's sensitivity in the validation group decreased to 32.4%, with specificity of 80.6%. The diagnostic accuracies of two models were statistically different ( $p < 0.05$ ) in both the training and validation cohort, with the RF model consistently outperforming the Nomogram model.

In addition, the DCA indicated that the curve of RF model consistently outperformed the Nomogram

model curve in both the training (Fig. 2C) and validation cohorts (Fig. 2D), which demonstrated the enhanced predictive effects in the RF model compared with the Nomogram model. To further evaluate model performance, we assessed net reclassification improvement (NRI) and integrated discrimination improvement (IDI). As illustrated in Table 1, the NRI and IDI demonstrated a notable improvement in training cohort (NRI% 100.0,  $p < 0.001$ ; IDI% 100.0,  $p < 0.001$ ) and validation cohort (NRI% 44.0,  $p < 0.001$ ; IDI% 36.1,  $p < 0.001$ ). These results demonstrated that RF model had a remarkable predictive capability compared to Nomogram model.

**Table 1** Evaluation of reclassification and discrimination improvement of the prediction models

| Prediction                 | IDI%               | <i>p</i> | NRI%                | <i>p</i> |
|----------------------------|--------------------|----------|---------------------|----------|
| Training cohorts           |                    |          |                     |          |
| RF model vs nomogram model | 100.0 (99.8–100.0) | <0.001   | 100.0 (100.0–100.0) | <0.001   |
| Validation cohorts         |                    |          |                     |          |
| RF model vs nomogram model | 36.1 (25.3–46.8)   | <0.001   | 44.0 (25.1–62.9)    | <0.001   |

*NRI* net reclassification improvement index, *IDI* integrated discrimination improvement index

Finally, we plotted clinical impact curves (CIC) for the RF model and the Nomogram model to assess their clinical effectiveness and applicability. In the training cohort, the RF model displayed a smoother CIC curve (Fig. 2E), exhibiting a higher number of high-risk individuals, especially at lower high-risk thresholds, highlighting its effectiveness in recognizing high-risk patients. In contrast, the Nomogram model showed relatively limited performance (Fig. 2F). However, in the validation cohort, the Nomogram model (Fig. 2H) exhibited more robust performance compared to the RF model (Fig. 2G).

### The performance of the predictive model in predicting prognosis in ICIs

To assess the prognostic predictive ability, we compared the C-index of the RF model with that of the Nomogram model, LIPI, and SIS.

As shown in Table 2 and Fig. 3A, B, the C-index of OS for the RF prediction model was 0.803 (95% CI 0.763–0.843), which was the highest in the training cohort ( $p < 0.001$ ) for Nomogram model (0.507, 95% CI 0.448–0.566), SIS (0.541, 95% CI 0.488–0.593) and LIPI (0.534, 95% CI 0.488–0.580). Similar outcomes were noticed in the validation cohort, with the RF model having the highest C-index (0.712, 95% CI 0.652–0.772) compared to Nomogram model (0.501, 95% CI 0.415–0.586), SIS (0.557, 95% CI 0.497–0.618) and LIPI (0.501, 95% CI 0.442–0.560).

For PFS, as displayed in Table 2 and Fig. 3C, D, the C-index of RF model for PFS was 0.663 (95% CI 0.617–0.710), and it exceeded that of the Nomogram model (0.502, 95% CI 0.455–0.549), SIS (0.508, 95% CI 0.461–0.555) and LIPI (0.528, 95% CI 0.492–0.565) in training cohort ( $p < 0.001$ ). In the validation cohort, the RF model had the highest C-index (0.711, 95% CI 0.658–0.765) among the Nomogram model (0.511, 95% CI 0.443–0.580), SIS (0.515, 95% CI 0.453–0.577) and LIPI (0.512, 95% CI 0.462–0.562).

These findings collectively highlight the superior predictive performance of the RF model for both OS and PFS compared to traditional prognostic models.

### Risk stratification of PFS/OS based on the prediction model

As shown in Table 3, patients were separated into high-risk and low-risk groups by the RF model. The K–M survival analysis revealed that individuals categorized as low-risk experienced a longer PFS compared to their high-risk counterparts in both the training and validation cohorts ( $p < 0.001$ ; Fig. 4A, B). However, the same trend was not observed in the Nomogram model (Fig. 4C, D). We also compared the K–M survival curves of the SIS and LIPI scores at 0, 1, and 2 points in the training and validation cohorts. What was observed indicated that

**Table 2** The C-index of OS/PFS for RF model, Nomogram, SIS, and LIPI

| Survival prediction        | C-index | 95 CI%      | <i>p</i> |
|----------------------------|---------|-------------|----------|
| Training cohort            |         |             |          |
| OS                         |         |             |          |
| RF model                   | 0.803   | 0.763–0.843 |          |
| Nomogram model             | 0.507   | 0.448–0.566 |          |
| SIS                        | 0.541   | 0.488–0.593 |          |
| LIPI                       | 0.534   | 0.488–0.580 |          |
| RF model vs Nomogram model |         |             | <0.001   |
| RF model vs SIS            |         |             | <0.001   |
| RF model vs LIPI           |         |             | <0.001   |
| PFS                        |         |             |          |
| RF model                   | 0.663   | 0.617–0.710 |          |
| Nomogram model             | 0.502   | 0.455–0.549 |          |
| SIS                        | 0.508   | 0.461–0.555 |          |
| LIPI                       | 0.528   | 0.492–0.565 |          |
| RF model vs Nomogram model |         |             | <0.001   |
| RF model vs SIS            |         |             | <0.001   |
| RF model vs LIPI           |         |             | <0.001   |
| Validation cohort          |         |             |          |
| OS                         |         |             |          |
| RF model                   | 0.712   | 0.652–0.772 |          |
| Nomogram model             | 0.501   | 0.415–0.586 |          |
| SIS                        | 0.557   | 0.497–0.618 |          |
| LIPI                       | 0.501   | 0.442–0.560 |          |
| RF model vs Nomogram model |         |             | <0.001   |
| RF model vs SIS            |         |             | <0.001   |
| RF model vs LIPI           |         |             | <0.001   |
| PFS                        |         |             |          |
| RF model                   | 0.711   | 0.658–0.765 |          |
| Nomogram model             | 0.511   | 0.443–0.580 |          |
| SIS                        | 0.515   | 0.453–0.577 |          |
| LIPI                       | 0.512   | 0.462–0.562 |          |
| RF model vs Nomogram model |         |             | <0.001   |
| RF model vs SIS            |         |             | <0.001   |
| RF model vs LIPI           |         |             | <0.001   |

The concordance index is denoted as C-index. *P* values are computed by applying the function `rcorr.cens` in the `Hmisc` package, based on normal approximation

LIPI showed a significant difference in PFS in the training cohort (Fig. 4G,  $p < 0.05$ ), while no significant difference was observed in the validation cohort (Fig. 4H). Conversely, SIS did not demonstrate any significant differences in either the training or validation cohorts (Fig. 4E, F).

We also did survival prognostic analysis of RF model, Nomogram model, SIS score, LIPI score with OS. The K–M survival curves indicated that in both the training (Fig. 4I) and validation cohorts (Fig. 4J), patients

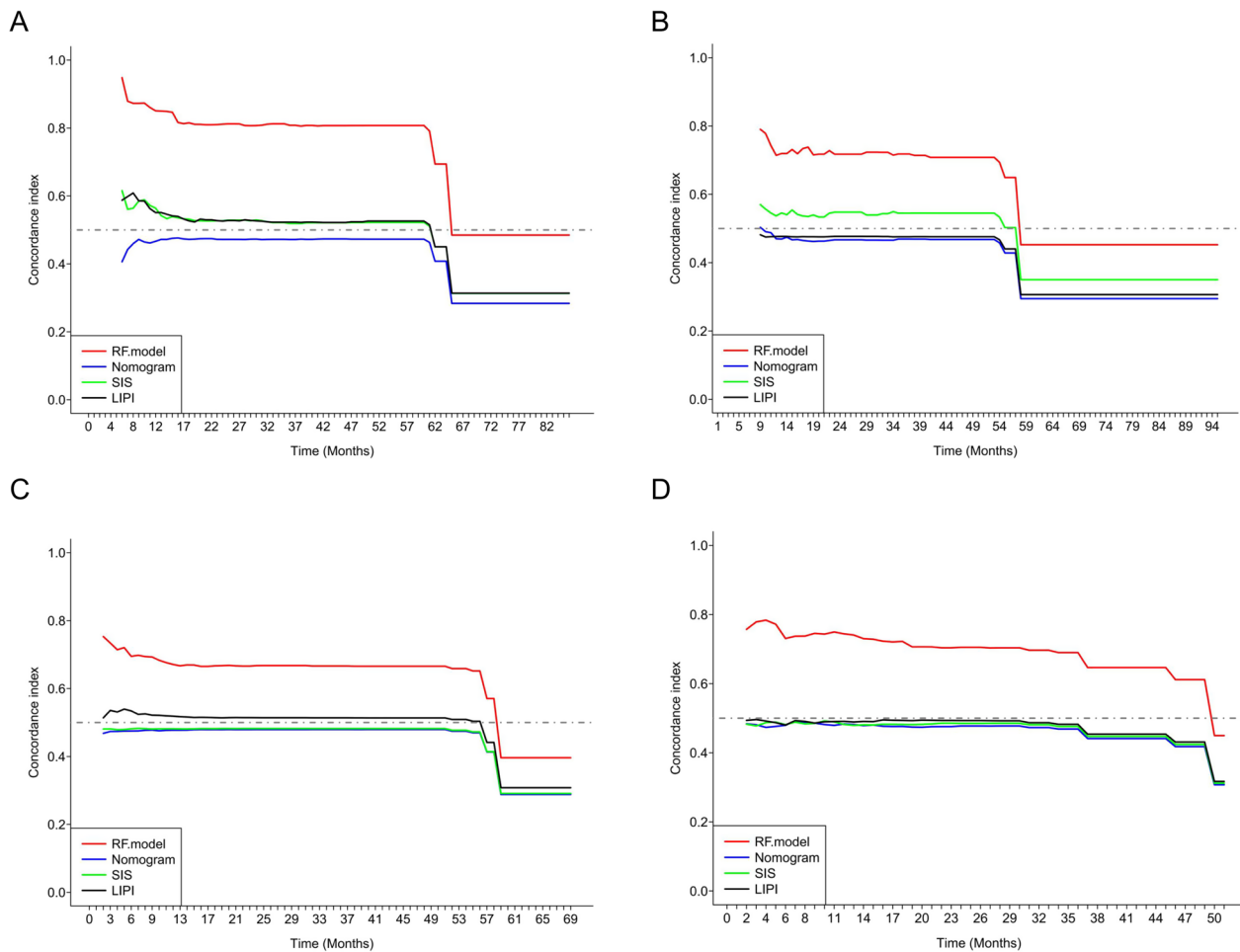


**Fig. 3** The C-index of OS for RF model, Nomogram, SIS and LIPI in training cohort (A) and validation cohort (B). The C-index of PFS for RF model, Nomogram, SIS and LIPI in training cohort (C) and validation cohort (D)

**Table 3** Response to ICIs therapy based on the RF model

| Survival prediction           | Low Risk  | High Risk | $\chi^2$ | $p$    |
|-------------------------------|-----------|-----------|----------|--------|
| For training cohort (n=)      | n=92      | n=122     |          |        |
| Best overall response-no. (%) |           |           | 19.31    | <0.001 |
| Complete Response (CR)        | 6 (6.5)   | 1 (0.8)   |          |        |
| Partial response (PR)         | 34 (37.0) | 32 (26.2) |          |        |
| Stable disease (SD)           | 35 (38.0) | 35 (28.7) |          |        |
| Progressive disease (PD)      | 17 (18.5) | 54 (44.3) |          |        |
| For validation cohort (n=)    | n=37      | n=68      |          |        |
| Best overall response-no. (%) |           |           | 11.212   | 0.006  |
| Complete Response (CR)        | 1 (2.7)   | 1 (1.5)   |          |        |
| Partial response (PR)         | 17 (45.9) | 25 (36.8) |          |        |
| Stable disease (SD)           | 15 (40.5) | 15 (22.1) |          |        |
| Progressive disease (PD)      | 4 (10.8)  | 27 (39.7) |          |        |

classified as low-risk exhibit significantly longer OS compared to high-risk patients ( $p < 0.001$ ). However, this trend was not observed in the Nomogram model (Fig. 4K, L), where no significant divergence in OS was observed between the high-risk and low-risk groups (Fig. 4K:  $p = 0.39$ ; Fig. 4L:  $p = 0.64$ ). Additionally, survival analyses based on SIS and LIPI scores revealed no significant differences in OS across the respective groups (SIS: Fig. 4M,  $p = 0.41$ ; Fig. 4N,  $p = 0.26$ ; LIPI: Fig. 4O,  $p = 0.11$ ; Fig. 4P,  $p = 0.95$ ). These findings suggested that while risk stratification using the RF model was predictive of OS, the nomogram model, SIS and LIPI did not exhibit the same level of prognostic differentiation.

Moreover, we conducted an analysis on the differences regarding the values of RDW-SD, MCV, PDW, CD3<sup>+</sup>CD8<sup>+</sup>, APTT, P-LCR, Ca, MPV, CD4<sup>+</sup>/CD8<sup>+</sup> and AST between the high-risk and low-risk groups (Fig. 5). In the training cohort, MCV ( $p = 0.003$ ), Ca ( $p = 0.019$ ), CD4<sup>+</sup>/CD8<sup>+</sup> ( $p = 0.002$ ), CD3<sup>+</sup>CD8<sup>+</sup> ( $p = 0.044$ ), MPV

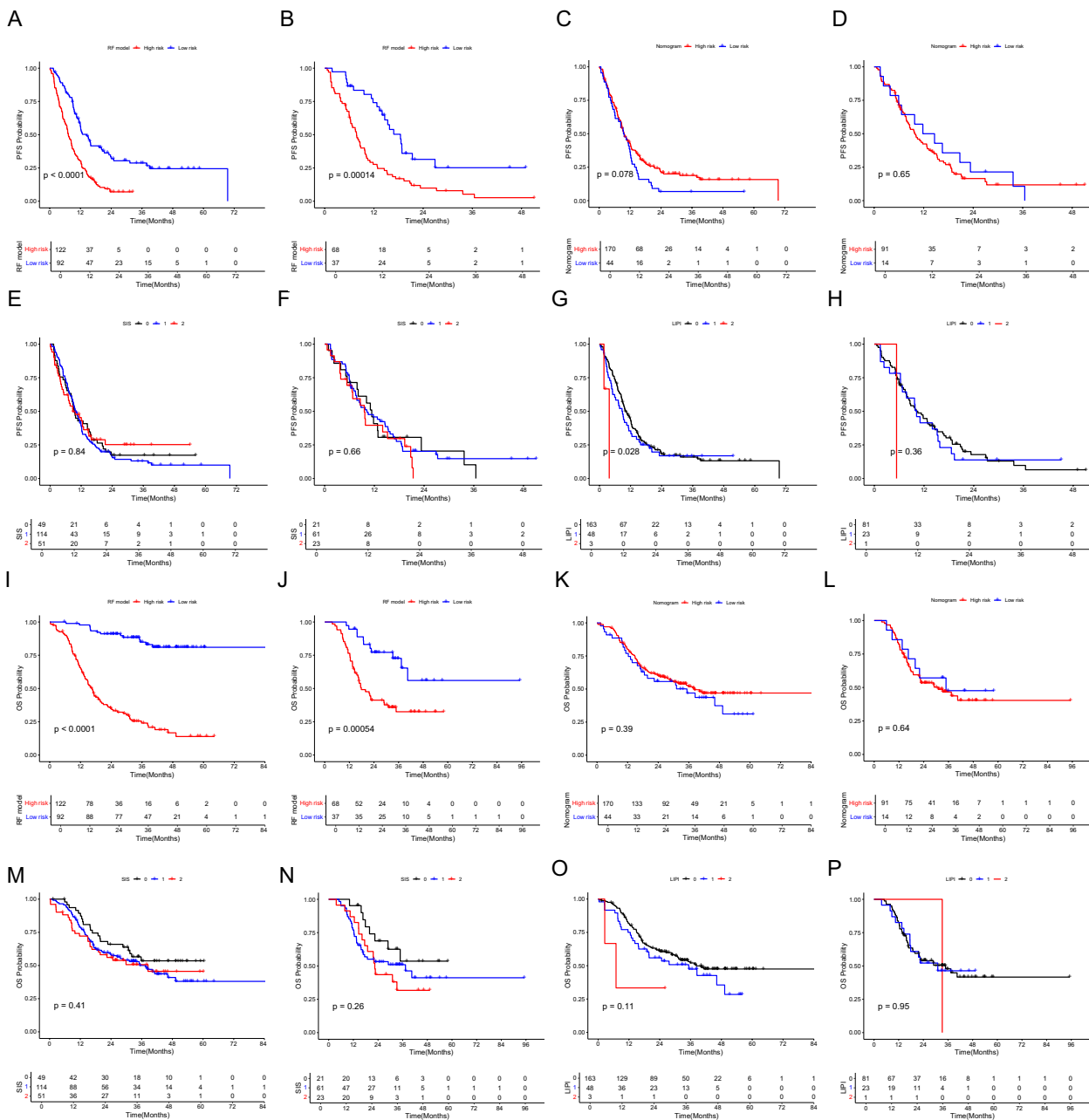


**Fig. 4** Risk categorization for PFS/OS in light of the prediction model. **A–H.** K–M survival curves for PFS of NSCLC Patients in the high-risk and low-risk groups in the Training Cohort (**A, C**) and Validation Cohort (**B, D**) in the RF Model and Nomogram model. K–M survival curves for PFS of NSCLC patients categorized by SIS score (0, 1, 2) in the training cohort (**E, G**) and validation cohort (**F, H**). **L–P.** K–M survival curves for OS of NSCLC Patients in the high-risk and low-risk groups in the Training Cohort (**I, K**) and Validation Cohort (**J, L**) in the RF Model and Nomogram model. K–M survival curves for OS of NSCLC patients categorized by SIS score (0, 1, 2), LIPI score (0, 1, 2) in the training cohort (**M, O**) and validation cohort (**N, P**)

( $p < 0.001$ ), PDW ( $p < 0.001$ ), P-LCR ( $p < 0.001$ ), and APTT ( $p = 0.005$ ) in the high-risk group differed significantly from those in the low-risk group. For the validation cohort, significant variations in RDW-SD ( $p = 0.004$ ) and APTT ( $p = 0.038$ ) existed between the high-risk group and the low-risk group.

### Discussion

In this study, based on routine blood tests (lymphocyte subpopulations, biochemical indexes and complete blood count), we utilized random forest algorithm to select ten predictive indicators (RDW-SD, MCV, PDW, CD3<sup>+</sup>CD8<sup>+</sup>, APTT, P-LCR, Ca, MPV, CD4<sup>+</sup>/CD8<sup>+</sup> ratio and AST),

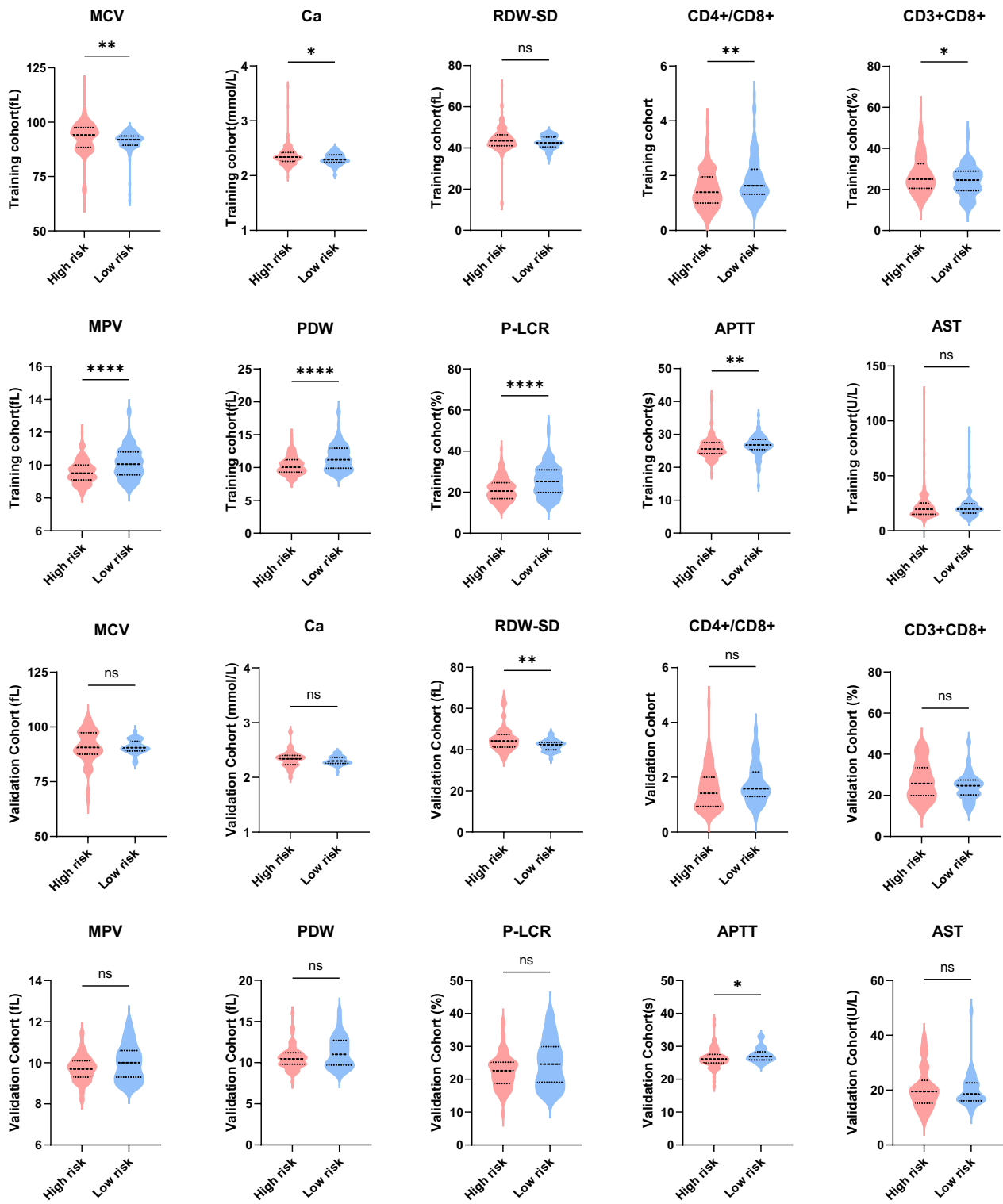


**Fig. 5** The differences in the number of RDW-SD, MCV, PDW, CD3<sup>+</sup>CD8<sup>+</sup>, APTT, P-LCR, Ca, MPV, CD4<sup>+</sup>/CD8<sup>+</sup> and AST between the high-risk and low-risk groups

and then constructed a RF model. We demonstrated that the RF model can not only predict the immune response but also predict the prognosis in NSCLC patients.

The predictive model selected two variables from lymphocyte subpopulations, including the CD4<sup>+</sup>/CD8<sup>+</sup> ratio and an immune cell subset (CD3<sup>+</sup>CD8<sup>+</sup>). CD4 and CD8 serve as markers for T helper (Th) and T suppressor (Ts) cell functions, respectively. The CD4<sup>+</sup>/CD8<sup>+</sup> ratio is a significant indicator of immune function, with an increased ratio suggesting enhanced Th cell function relative to Ts cells and improved immune activity. Studies have confirmed that the quantity of the CD8<sup>+</sup>/CD4<sup>+</sup> ratio in the TME correlates with prognosis in bladder cancer or melanoma patients undergoing ICIs treatment and can serve as a positive predictive factor for immunotherapy outcomes [34, 35]. In addition, it has been shown that CD3<sup>+</sup> and CD8<sup>+</sup> T-cell densities in tumors are positively correlated with OS and PFS [36]. The TME significantly influences tumor progression. Inflammatory responses, triggered by the release of cytokines, lead to abnormal cell proliferation and promote tumorigenesis. Numerous inflammatory blood cell markers and nutritional indicators have been linked to tumor prognosis [37]. In this study, we focused on two red blood cell-related indicators: RDW-SD and MCV. RDW-SD is defined as the width of the red blood cell volume distribution curve exceeding the baseline by more than 20%. Previous studies [38] have demonstrated that RDW-SD is closely associated with oxidative stress, inflammatory responses, and malnutrition. As a marker of red blood cell heterogeneity, RDW-SD has been identified as an independent prognostic factor in NSCLC [39], and its elevation correlates with poor outcomes in lung cancer [37], colorectal cancer [40], breast cancer [41], and gastric cancer [42]. MCV reflects the size of red blood cells and has clinical significance. Studies have reported that lower MCV values indicate more severe anemia and inflammation. This condition often contributes to cancer-related anemia (CAR) in malignancies such as colorectal cancer [43] and gastric cancer, further impairing patients' physical function, treatment tolerance, and prognosis. The balance between coagulation and anticoagulation systems is essential for maintaining homeostasis. Disruption of this balance increases the risk of thrombotic diseases and exacerbates lung cancer progression or metastasis. Recent findings [44] highlight the role of platelets not only in coagulation cascades but also in inflammation and tumor development. Activated platelets support tumor growth, angiogenesis, and invasion. Indicators such as PDW, P-LCR, and MPV, which reflect platelet activation and turnover, play crucial roles in tumor progression and immune regulation. In NSCLC [45], reduced PDW is an adverse prognostic marker. Higher

baseline MPV has been associated with better outcomes in NSCLC patients undergoing immunotherapy, including longer PFS and OS [46]. Larger platelets, characterized by higher enzymatic activity, release pro-thrombotic and pro-inflammatory factors, potentially leading to disease-specific complications [47]. A decline in P-LCR in malignancies has been correlated with worse OS [48], potentially due to increased tumor-associated platelet activation, driving cancer progression and poor prognosis. Coagulation abnormalities often manifest as platelet hyperactivation and pathway dysregulation. Prolonged APTT, an indicator of intrinsic coagulation pathway dysfunction, has been reported to be associated with poor OS in NSCLC [49]. Calcium ions (Ca<sup>2+</sup>) serve as ubiquitous signaling molecules, orchestrating key processes in cancer, including proliferation, apoptosis, migration, and immune response [50]. Dysregulated Ca<sup>2+</sup> homeostasis has emerged as a critical Promoter of tumor growth and influences treatment outcomes [51].

In this study, the constructed RF model demonstrates strong generalization capability and robust predictive performance. When faced with numerous features in routine blood tests, the random forest algorithm can automatically assess the importance of these features for predicting the efficacy of ICIs therapy and accurately identify key variables. Compared to traditional Nomogram model, LIPI, SIS, the RF model exhibits superior predictive performance. Although Nomogram model is user-friendly for clinicians, they depend heavily on data quality. LIPI and SIS, as biomarkers built on specific clinical indicators, have the advantage of being simple to use; however, their relatively singular nature may fail to comprehensively reflect the patient's condition. The RF model, on the other hand, has advantages in handling high-dimensional data, requiring less stringent assumptions about data distribution, and demonstrating good generalization capabilities. Peripheral blood biomarkers offer advantages such as minimally invasive sampling, potential reproducibility, and the ability for sequential monitoring, and they have been shown to be promising tools for predicting responses to immunotherapy. The RF model based on hematological parameters can provide a rapid and cost-effective way to deliver more scientifically reliable predictions regarding ICIs therapy outcomes. Additionally, the risk scores generated from the RF model can offer valuable references for the prognosis of patients undergoing ICIs therapy.

Despite the achievements of this study, several limitations in our study should be noted. Firstly, this is a retrospective study, which may lead to unavoidable selection bias in the data. Secondly, it is a single-center study, with data derived solely from internal sources, lacking external validation. Finally, the study did not incorporate other

tumor biomarkers, such as exosomal protein, ctDNA, and miRNA. In future research, we aim to collaborate with other hospitals to increase the sample size and attempt to include diverse data.

## Conclusion

In summary, we developed a novel prognostic random forest model (RF model) based on routine blood tests and highlighted its significance as potential prognostic biomarkers for patients undergoing ICIs therapy for NSCLC. The RF model is an important tool for identifying the beneficiaries of ICIs therapy in NSCLC. Therefore, in future studies, we need to conduct multi-center, large-sample, prospective clinical trials to further optimize and evaluate the predictive performance of the model.

## Abbreviations

|        |   |
|--------|---|
| ICIs   | Immune checkpoint inhibitors                |
| NSCLC  | Non-small cell lung cancer                  |
| ROC    | Receiver operating characteristic           |
| K-M    | K-M survival curves                         |
| CIC    | Clinical impact curve                       |
| DCA    | Decision curve analysis                     |
| SCLC   | Small cell lung cancer                      |
| PD-L1  | Programmed cell death ligand 1              |
| CTLA-4 | Cytotoxic T lymphocyte-associated antigen 4 |
| PD-1   | Programmed cell death receptor 1            |

## Supplementary Information

The online version contains supplementary material available at <https://doi.org/10.1186/s12935-025-03800-3>.

Additional file 1.

## Acknowledgements

The authors thank our patients at the Sun Yat-Sen University Cancer Center who donated clinical data for this study.

## Author contributions

TZ and XL contributed equally to this work. SC, YZ and ZL conceived this study, and they are the corresponding authors. TZ, XL and YM designed the experiments, performed data analysis, and wrote the draft manuscript. JL and WL provided patient recruitment and sample collection.

## Funding

The Project for Traditional Chinese Medicine of National Heritage and Innovation Center (2022ZD07).

## Data availability

The datasets used or analyzed during the current study are available from the corresponding author on reasonable request.

## Declarations

### Ethics approval and consent to participate

Approval for this study was granted by the Institute Research Ethics Committee of the Sun Yat-Sen University Cancer Center (Guangzhou, China; Approval No. B2024-848-01). Written informed consent was exempted because of retrospective analysis. This study was conducted in accordance with the Declaration of Helsinki and patient confidentiality is guaranteed.

## Consent for publication

Not applicable.

## Competing interests

The authors declare no competing interests.

## Author details

<sup>1</sup>The First Clinical Medical College and the First Affiliated Hospital of Guangzhou University of Chinese Medicine, Guangzhou 510405, Guangdong, People's Republic of China. <sup>2</sup>The First Affiliated Hospital of Guangzhou University of Chinese Medicine, Guangzhou 510405, Guangdong, People's Republic of China. <sup>3</sup>Baiyun Hospital of The First Affiliated Hospital of Guangzhou University of Chinese Medicine, Guangzhou 510470, Guangdong, People's Republic of China. <sup>4</sup>Department of Clinical Laboratory, State Key Laboratory of Oncology in South China, Guangdong Key Laboratory of Nasopharyngeal Carcinoma Diagnosis and Therapy, Guangdong Provincial Clinical Research Center for Cancer, Sun Yat-Sen University Cancer Center, 651 Dongfeng Road East, Guangzhou 510060, Guangdong, People's Republic of China.

Received: 20 January 2025 Accepted: 24 April 2025

Published online: 15 May 2025

## References

- Siegel RL, Giaquinto AN, Jemal A. Cancer statistics, 2024. *CA Cancer J Clin*. 2024;74(1):12–49.
- Zhang Y, Wang DC, Shi L, Zhu B, Min Z, Jin J. Genome analyses identify the genetic modification of lung cancer subtypes. *Semin Cancer Biol*. 2017;42:20–30.
- Bagchi S, Yuan R, Engleman EG. Immune checkpoint inhibitors for the treatment of cancer: clinical impact and mechanisms of response and resistance. *Annu Rev Pathol*. 2021;16:223–49.
- Hodi FS, Chiarion-Sileni V, Gonzalez R, Grob JJ, Rutkowski P, Cowey CL, Lao CD, Schadendorf D, Wagstaff J, Dummer R, et al. Nivolumab plus ipilimumab alone versus ipilimumab alone in advanced melanoma (CheckMate 067): 4-year outcomes of a multicentre, randomised, phase 3 trial. *Lancet Oncol*. 2018;19(11):1480–92.
- Burtress B, Harrington KJ, Greil R, Soulieres D, Tahara M, de Castro G Jr, Psyrri A, Baste N, Neupane P, Bratland A, et al. Pembrolizumab alone or with chemotherapy versus cetuximab with chemotherapy for recurrent or metastatic squamous cell carcinoma of the head and neck (KEYNOTE-048): a randomised, open-label, phase 3 study. *Lancet*. 2019;394(10212):1915–28.
- Fradet Y, Bellmunt J, Vaughn DJ, Lee JL, Fong L, Vogelzang NJ, Climent MA, Petrylak DP, Choueiri TK, Necchi A, et al. Randomized phase III KEYNOTE-045 trial of pembrolizumab versus paclitaxel, docetaxel, or vinflunine in recurrent advanced urothelial cancer: results of >2 years of follow-up. *Ann Oncol*. 2019;30(6):970–6.
- Escudier B, Sharma P, McDermott DF, George S, Hammers HJ, Srinivas S, Tykodi SS, Sosman JA, Procopio G, Plimack ER, et al. CheckMate 025 randomized phase 3 study: outcomes by key baseline factors and prior therapy for nivolumab versus everolimus in advanced renal cell carcinoma. *Eur Urol*. 2017;72(6):962–71.
- Reck M, Rodriguez-Abreu D, Robinson AG, Hui R, Czoszi T, Fulop A, Gottfried M, Peled N, Tafreshi A, Cuffe S, et al. Five-Year outcomes with pembrolizumab versus chemotherapy for metastatic non-small-cell lung cancer with PD-L1 tumor proportion score  $\geq$  50. *J Clin Oncol*. 2021;39(21):2339–49.
- Riely GJ, Wood DE, Ettinger DS, Aisner DL, Akerley W, Bauman JR, Bharat A, Bruno DS, Chang JY, Chirieac LR, et al. Non-small cell lung cancer, version 4.2024. NCCN clinical practice guidelines in oncology. *J Natl Compr Canc Netw*. 2024;22(4):249–74.
- Robert C, Ribas A, Schachter J, Arance A, Grob JJ, Mortier L, Daud A, Carlino MS, McNeil CM, Lotem M, et al. Pembrolizumab versus ipilimumab in advanced melanoma (KEYNOTE-006): post-hoc 5-year results from an open-label, multicentre, randomised, controlled, phase 3 study. *Lancet Oncol*. 2019;20(9):1239–51.
- Schoenfeld AJ, Rizvi H, Bandlamudi C, Sauter JL, Travis WD, Rekhman N, Plodkowski AJ, Perez-Johnston R, Sawan P, Beras A, et al. Clinical and

- molecular correlates of PD-L1 expression in patients with lung adenocarcinomas. *Ann Oncol.* 2020;31(5):599–608.
12. Wang Z, Duan J, Cai S, Han M, Dong H, Zhao J, Zhu B, Wang S, Zhuo M, Sun J, et al. Assessment of blood tumor mutational burden as a potential biomarker for immunotherapy in patients with non-small cell lung cancer with use of a next-generation sequencing cancer gene panel. *JAMA Oncol.* 2019;5(5):696–702.
  13. Mathew M, Zade M, Mezghani N, Patel R, Wang Y, Momen-Heravi F. Extracellular vesicles as biomarkers in cancer immunotherapy. *Cancers.* 2020;12(10):2825.
  14. Keegan A, Ricciuti B, Garden P, Cohen L, Nishihara R, Adeni A, Paweletz C, Supplee J, Janne PA, Severgnini M, et al. Plasma IL-6 changes correlate to PD-1 inhibitor responses in NSCLC. *J Immunother Cancer.* 2020;8(2):e000678.
  15. Yuen KC, Liu LF, Gupta V, Madireddi S, Keerthivasan S, Li C, Rishipathak D, Williams P, Kadel EE 3rd, Koepfen H, et al. Author correction: high systemic and tumor-associated IL-8 correlates with reduced clinical benefit of PD-L1 blockade. *Nat Med.* 2021;27(3):560.
  16. Paijens ST, Vledder A, de Bruyn M, Nijman HW. Tumor-infiltrating lymphocytes in the immunotherapy era. *Cell Mol Immunol.* 2021;18(4):842–59.
  17. Sade-Feldman M, Yizhak K, Bjorgaard SL, Ray JP, de Boer CG, Jenkins RW, Lieb DJ, Chen JH, Frederick DT, Barzily-Rokni M, et al. Defining T cell states associated with response to checkpoint immunotherapy in melanoma. *Cell.* 2018;175(4):998–1013.e1020.
  18. An HJ, Chon HJ, Kim C. Peripheral blood-based biomarkers for immune checkpoint inhibitors. *Int J Mol Sci.* 2021;22(17):9414.
  19. Chen DS, Mellman I. Elements of cancer immunity and the cancer-immune set point. *Nature.* 2017;541(7637):321–30.
  20. Hegde PS, Karanikas V, Evers S. The where, the when, and the how of immune monitoring for cancer immunotherapies in the era of checkpoint inhibition. *Clin Cancer Res.* 2016;22(8):1865–74.
  21. Galon J, Bruni D. Approaches to treat immune hot, altered and cold tumours with combination immunotherapies. *Nat Rev Drug Discov.* 2019;18(3):197–218.
  22. Herbst RS, Soria JC, Kowanzet M, Fine GD, Hamid O, Gordon MS, Sosman JA, McDermott DF, Powderly JD, Gettinger SN, et al. Predictive correlates of response to the anti-PD-L1 antibody MPDL3280A in cancer patients. *Nature.* 2014;515(7528):563–7.
  23. Hayashi H, Chamoto K, Hatae R, Kurosaki T, Togashi Y, Fukuoka K, Goto M, Chiba Y, Tomida S, Ota T, et al. Soluble immune checkpoint factors reflect exhaustion of antitumor immunity and response to PD-1 blockade. *J Clin Invest.* 2024;134(7).
  24. Wang Z, Wu L, Li B, Cheng Y, Li X, Wang X, Han L, Wu X, Fan Y, Yu Y, et al. Toripalimab plus chemotherapy for patients with treatment-naïve advanced non-small-cell lung cancer: a multicenter randomized phase III trial (CHOICE-01). *J Clin Oncol.* 2023;41(3):651–63.
  25. Tang B, Chen Y, Jiang Y, Fang M, Gao Q, Ren X, Yao L, Huang G, Chen J, Zhang X, et al. Toripalimab in combination with HBM4003, an anti-CTLA-4 heavy chain-only antibody, in advanced melanoma and other solid tumors: an open-label phase I trial. *J Immunother Cancer.* 2024;12(10):e009662.
  26. Choueiri TK, Kluger H, George S, Tykodi SS, Kuzel TM, Perets R, Nair S, Procopio G, Carducci MA, Castonguay V, et al. FRACTION-RCC: nivolumab plus ipilimumab for advanced renal cell carcinoma after progression on immuno-oncology therapy. *J Immunother Cancer.* 2022;10(11):e005780.
  27. Liu Z, Meng X, Tang X, Zou W, He Y. Intratumoral tertiary lymphoid structures promote patient survival and immunotherapy response in head neck squamous cell carcinoma. *Cancer Immunol Immunother.* 2023;72(6):1505–21.
  28. Ullman NA, Burchard PR, Dunne RF, Linehan DC. Immunologic strategies in pancreatic cancer: making cold tumors hot. *J Clin Oncol.* 2022;40(24):2789–805.
  29. Chiocca EA, Gelb AB, Chen CC, Rao G, Reardon DA, Wen PY, Bi WL, Peruzzi P, Amidei C, Triggs D, et al. Combined immunotherapy with controlled interleukin-12 gene therapy and immune checkpoint blockade in recurrent glioblastoma: an open-label, multi-institutional phase I trial. *Neuro Oncol.* 2022;24(6):951–63.
  30. Zhang K, Liu K, Hu B, Du G, Chen X, Xiao L, Zhang Y, Jiang L, Jing N, Cheng C, et al. Iron-loaded cancer-associated fibroblasts induce immunosuppression in prostate cancer. *Nat Commun.* 2024;15(1):9050.
  31. Wang X, Guo Z, Wu X, Chen D, Wang F, Yang L, Luo M, Wu S, Yang C, Huang L, et al. Predictive nomogram for hyperprogressive disease during anti-PD-1/PD-L1 treatment in patients with advanced non-small cell lung cancer. *Immunotargets Ther.* 2023;12:1–16.
  32. Menyhart O, Fekete JT, Györfy B. Inflammation and colorectal cancer: a meta-analysis of the prognostic significance of the systemic immune-inflammation index (SII) and the systemic inflammation response index (SIRI). *Int J Mol Sci.* 2024;25(15):8441.
  33. Chen YR, Chen YL, Ouyang SS, Xu HW, Li P, He LJ, Zhu SL. Prognostic efficacy of preoperative mGPS, SJS and LCS in patients with gastric cancer. *Clin Chim Acta.* 2020;511:81–9.
  34. Chen X, Xu R, He D, Zhang Y, Chen H, Zhu Y, Cheng Y, Liu R, Zhu R, Gong L, et al. CD8(+) T effector and immune checkpoint signatures predict prognosis and responsiveness to immunotherapy in bladder cancer. *Oncogene.* 2021;40(43):6223–34.
  35. Jiang P, Gu S, Pan D, Fu J, Sahu A, Hu X, Li Z, Traugh N, Bu X, Li B, et al. Signatures of T cell dysfunction and exclusion predict cancer immunotherapy response. *Nat Med.* 2018;24(10):1550–8.
  36. Sun X, Zhai J, Sun B, Parra ER, Jiang M, Ma W, Wang J, Kang AM, Kannan K, Pandureangan R, et al. Effector memory cytotoxic CD3(+)/CD8(+)/CD45RO(+) T cells are predictive of good survival and a lower risk of recurrence in triple-negative breast cancer. *Mod Pathol.* 2022;35(5):601–8.
  37. Lv X, Xu B, Zou Q, Han S, Feng Y. Clinical application of common inflammatory and nutritional indicators before treatment in prognosis evaluation of non-small cell lung cancer: a retrospective real-world study. *Front Med.* 2023;10:1183886.
  38. Salvagno GL, Sanchis-Gomar F, Picanza A, Lippi G. Red blood cell distribution width: a simple parameter with multiple clinical applications. *Crit Rev Clin Lab Sci.* 2015;52(2):86–105.
  39. Lochowski M, Chalubinska-Fendler J, Lochowska B, Zawadzka I, Brzezinski D, Rebowski M, Kozak J. Prognostic value of red blood cell distribution width-standard deviation (RDW-SD) in patients operated on due to non-small cell lung cancer. *J Thorac Dis.* 2020;12(3):773–81.
  40. Lu X, Huang X, Xue M, Zhong Z, Wang R, Zhang W, Wang L, Qiao Y, Ling F, Zhang Q, et al. Prognostic significance of increased preoperative red cell distribution width (RDW) and changes in RDW for colorectal cancer. *Cancer Med.* 2023;12(12):13361–73.
  41. Yin JM, Zhu KP, Guo ZW, Yi W, He Y, Du GC. Is red cell distribution width a prognostic factor in patients with breast cancer? A meta-analysis. *Front Surg.* 2023;10:1000522.
  42. Saito H, Shimizu S, Shishido Y, Miyatani K, Matsunaga T, Fujiwara Y. Prognostic significance of the combination of preoperative red cell distribution width and platelet distribution width in patients with gastric cancer. *BMC Cancer.* 2021;21(1):1317.
  43. Vayrynen JP, Tuomisto A, Vayrynen SA, Klintrup K, Karhu T, Makela J, Herzog KH, Karttunen TJ, Makinen MJ. Preoperative anemia in colorectal cancer: relationships with tumor characteristics, systemic inflammation, and survival. *Sci Rep.* 2018;8(1):1126.
  44. Franco AT, Corken A, Ware J. Platelets at the interface of thrombosis, inflammation, and cancer. *Blood.* 2015;126(5):582–8.
  45. Cui MM, Li N, Liu X, Yun ZY, Niu Y, Zhang Y, Gao B, Liu T, Wang RT. Platelet distribution width correlates with prognosis of non-small cell lung cancer. *Sci Rep.* 2017;7(1):3456.
  46. Krizova L, Benesova I, Zemanova P, Spacek J, Strizova Z, Humlova Z, Mikulova V, Petruzalka L, Vocka M. Immunophenotyping of peripheral blood in NSCLC patients discriminates responders to immune checkpoint inhibitors. *J Cancer Res Clin Oncol.* 2024;150(2):99.
  47. Halawi M. Prognostic value of evaluating platelet role, count and indices in laboratory diagnosis of different types of solid malignancies. *Pak J Biol Sci.* 2022;25(2):100–5.
  48. Chen Y, Yang W, Ye L, Lin S, Shu K, Yang X, Ai X, Yao Y, Jiang M. Economical and easily detectable markers of digestive tumors: platelet parameters. *Biomark Med.* 2021;15(3):157–66.
  49. Abbas M, Kassim SA, Wang ZC, Shi M, Hu Y, Zhu HL. Clinical evaluation of plasma coagulation parameters in patients with advanced-stage non-small cell lung cancer treated with palliative chemotherapy in China. *Int J Clin Pract.* 2020;74(12):e13619.
  50. Giorgi C, Danese A, Missiroli S, Patergnani S, Pinton P. Calcium dynamics as a machine for decoding signals. *Trends Cell Biol.* 2018;28(4):258–73.

51. Zheng S, Wang X, Zhao D, Liu H, Hu Y. Calcium homeostasis and cancer: insights from endoplasmic reticulum-centered organelle communications. *Trends Cell Biol.* 2023;33(4):312–23.

### **Publisher's Note**

Springer Nature remains neutral with regard to jurisdictional claims in published maps and institutional affiliations.